Rotational velocities of F dwarfs; application of the Fourier-Bessel transformation method

Groot, P.J.; Piters, A.J.M.; van Paradijs, J.A.

Publication date
1996

Published in
Astronomy and Astrophysics Supplement Series

ASTRONOMY & ASTROPHYSICS
SUPPLEMENT SERIES

Astron. Astrophys. Suppl. Ser. **118,** 545-555 (1996)

Rotational velocities of F dwarfs; application of the Fourier-Bessel transformation method*

P.J. Groot[1], A.J.M. Piters[1] and J. van Paradijs[1,2]

[1] Astronomical Institute 'Anton Pannekoek'/ CHEAF, Kruislaan 403, 1098 SJ, Amsterdam, The Netherlands
[2] Physics Department, UAH, Huntsville, AL 35899, U.S.A.

Received November 22, 1994; accepted January 30, 1996

Abstract. — Projected rotational velocities are presented for 178 bright dwarf stars (V <7) with spectral types in the range A8 till G2. These rotational velocities have been determined by Fourier-Bessel transformation of the line profiles of six Fe I absorption lines in a 50 Å wide range centered on 6250 Å. Rotational velocities of stars with suspected velocities of more than 40 km/s were also determined by fitting the whole spectral range with a profile of a slowly rotating star of the same spectral type that has been convolved with a rotation profile. The agreement between the results obtained with these two methods is very good.**

Key words: line: profiles — stars: rotation — techniques: spectroscopic

1. Introduction

In order to study the effects of stellar rotation on magnetic activity, and its onset along the main sequence, we have collected a variety of data for a sample of 178 bright dwarfs with spectral type between A8 and G2. This range of spectral types has been chosen because magnetic activity (e.g., Walter 1983; Schmitt et al. 1985) is suspected to become important in mid F-type dwarfs, which is also indicated by the decline in average rotational velocity in this spectral region, well known from the work of Slettebak (1955), Herbig & Spelding (1953, 1955), Huang (1953) and Kraft (1965).

For this sample of stars we obtained Walraven photometry, from which we derived the effective temperature and surface gravity, and ROSAT All-Sky Survey X-ray data, a diagnostic for magnetic activity (Piters et al. 1995).

To study the effect of rotation, we determined rotational velocities using the Fourier-Bessel Transformation (FBT) method as described in Piters et al. (1995) (hereafter Paper I) and by fitting the spectra with those of slowly rotating stars of the same spectral type, convolved with a rotation profile, for a range of assumed rotational velocities.

In Sect. 2 we give an overview of our observations and their reduction. In Sect. 3 we describe the determination of the rotational velocities with the FBT method. Section 4 lists our results obtained with this method, Sect. 5 describes the determination of rotational velocities with the convolution method, and makes a comparison between the results of the two methods. In Sect. 6 we summarize our conclusions.

2. The observations and their reduction

Our stars consist of a sub-sample of all main-sequence stars with spectral types between A8 and G2, located between $14^h<\alpha<24^h$ and $0^h<\alpha<02^h$ and $\delta<+20°$, that are listed in the Bright Star Catalogue (BSC), (Hoffleit & Jaschek 1982) and for which this Catalogue does not give any indication of 'abnormalities' in spectral type, such as emission lines. Added to this sample are some stars that will serve as comparison stars for the rotational velocities to test the FBT method, but that will not be used in any further search for a correlation with magnetic activity. A list of stars, together with their visual magnitudes and projected rotational velocities is presented in Table 4. Table 1 gives the number of stars per spectral type for our sample of dwarfs.

For the determination of the rotational velocities we selected six Fe I absorption lines around 6250 Å. Figure 1 shows the position of these lines in the spectrum of HR 7605 (an F4V star, for which we derive a rotational velocity of $v\sin i \sim 12$ km s^{-1}. We selected these lines on the basis of synthetic spectra, obtained from Kurucz model atmospheres (1979, 1992) and spectral lines from Kurucz & Peytremann (1975). The synthetic spectra show that most

*Based on observations with the 1.4 m CAT telescope at ESO
**Table 4 is only available in electronic form at the CDS via anonymous ftp 130.79.128.5

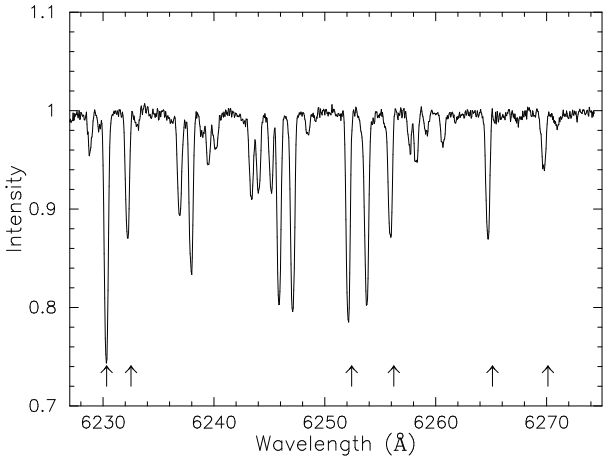

Fig. 1. The spectrum of the star HR 7605. The triangles indicate the lines used in the determination of the rotational velocity. No correction for radial velocity has been made

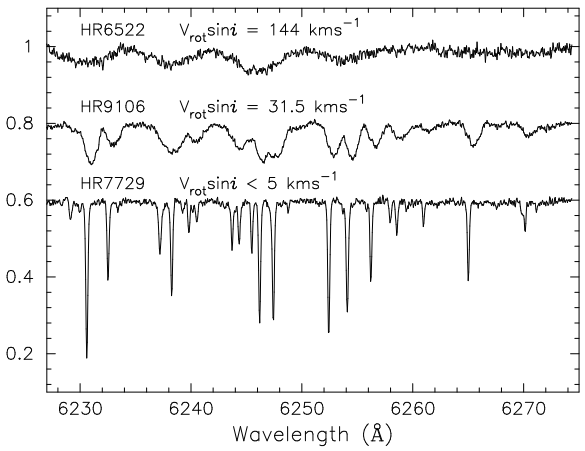

Fig. 2. The spectra of three F2V stars. The vertical scale has been shifted 0.2 between the three spectra. In these, and other spectra shown in this paper radial-velocity corrections to the wavelength scale have not been made

Table 1. Number of observed stars per spectral type

Spectral type	No. of stars	Spectral type	No. of stars
A8	4	F6	20
A9	2	F7	21
F0	16	F8	20
F1	5	F9	8
F2	14	G0	12
F3	12	G1	5
F4	10	G2	5
F5	15		

of the selected lines are visible in the whole spectral range A8-G2, and that they are reasonably clean. Detailed information on the selected lines is given below. These lines have also frequently been used by Gray (1981, 1982, 1989). The six lines lie rather close together, which made it possible to take high-resolution spectra and at the same time still have a sufficiently large number of lines available in the limited available wavelength range to make averaging of the rotational velocities of the different lines possible.

The lines that we used, and their properties in the spectral range considered (A8-G2) are:

λ 6230.728 Å: At later spectral types this line will blend with V I λ 6230.794.

λ 6232.649 Å: A reasonably clean line. In cool stars blending occurs with Co I λ 6232.437 and Ce I λ 6232.450. In hotter stars with rotational velocities above $\sim$30 km s^{-1} blending can occur with Al II λ 6231.718.

λ 6252.561 Å: A clean line that is still usable at high rotational velocities, as can be seen in Fig. 2. At later spectral types blending can occur with V I λ 6251.827.

λ 6256.367 Å: At later spectral types this line will blend with Si I λ 6256.448.

λ 6265.143 Å: The cleanest line. Towards cooler stars a line of Mn I appears at λ 6265.612 Å. This line could be affected by telluric water vapour. Any evidence of this water vapour would be especially clear in the spectra of the fast rotators, where it would show up as a narrow absorption feature. No evidence of this has been found. (See for instance Figs. 2, 12, 13 and 14.)

λ 6270.228 Å: A blend with Fe II λ 6269.982 is often visible, as can also be seen in Fig. 1. The Fe I line becomes weaker at earlier spectral types. This line is also the first to disappear at higher rotational velocities as can been seen in Fig. 2.

The spectra were obtained in two observing periods with the 1.4m Coudé Auxiliary Telescope at ESO La Silla. The first period was from July 26 to July 30, 1991, and the second from August 2 to August 6, 1992. The spectra have a resolution of 60.000 and S/N-ratios of at least 100. The covered wavelength region is from 6225 Å to 6277 Å. From the width of the Th-Ar calibration lines we estimate that the resolution in our spectra is $\sim$ 2 pixels (i.e. $\sim$0.1 Å).

The reduction was done using the ESO-MIDAS reduction package. Normal bias and flatfield corrections have been made. Bias frames and flatfield spectra were obtained three times each night. No sky subtraction has been performed because of the low sky intensities compared with those of the star ($< 1\%$). The wavelength calibration was done using Th-Ar spectra obtained during the observing periods. To achieve a normalized spectrum (one of the requirements of the FBT-method), the spectra were divided by their continuum, which was determined by fitting a third-order polynomial to at least ten points in the spectrum, selected by eye. Figure 2 shows three spectra of stars with spectral type F2. The top one is of HR 6522

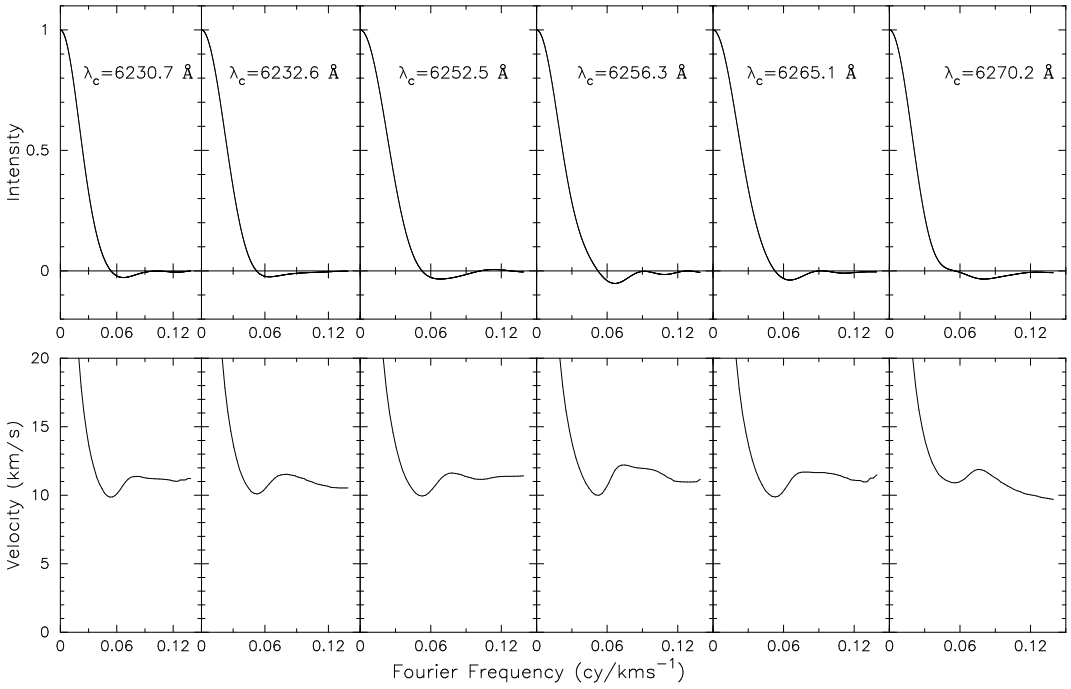

Fig. 3. Top panel: The Fourier transforms of the six lines of the star HR7605. Bottom panel: The vcf-plots of these six lines

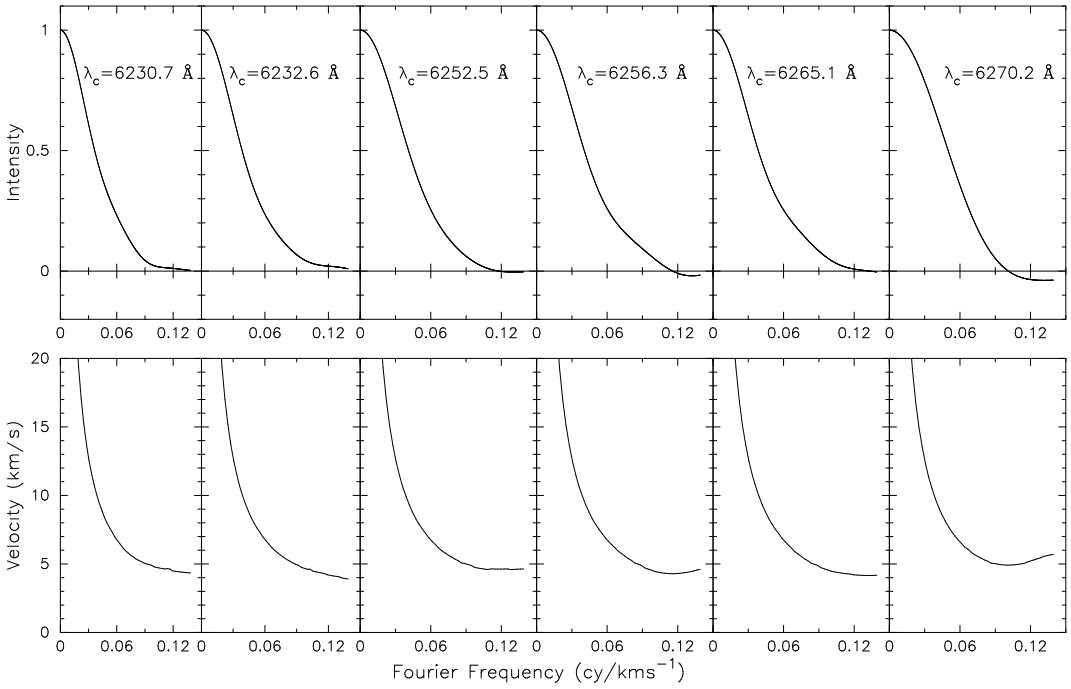

Fig. 4. Top panel: The Fourier transforms of the six lines of the star HR7729. Bottom panel: The vcf-plots of these six lines

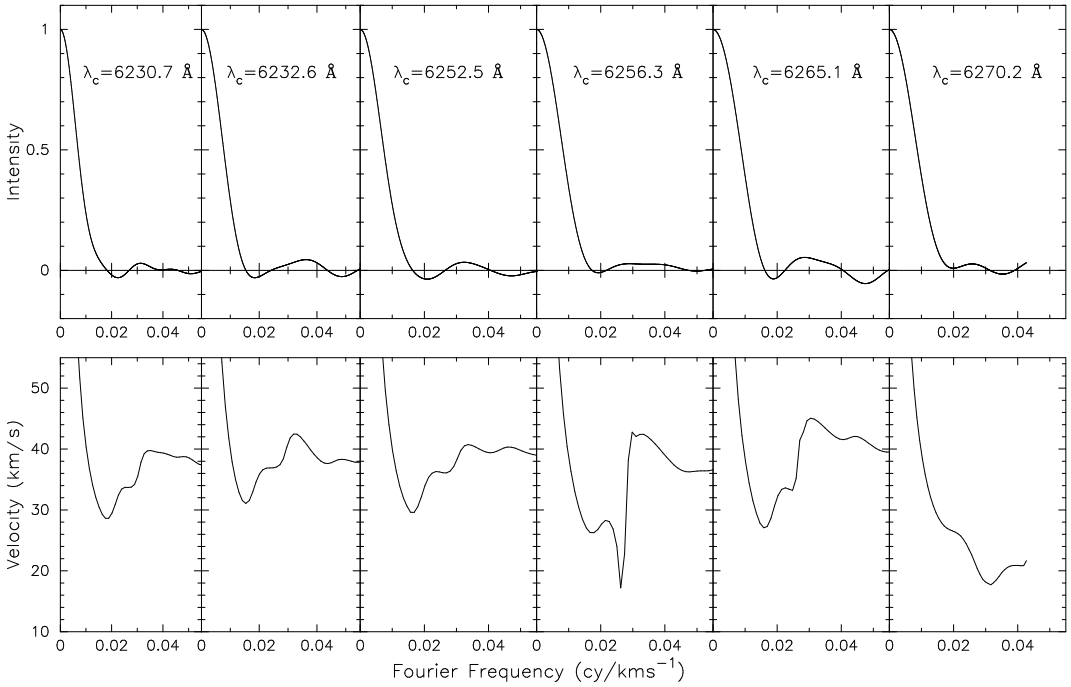

Fig. 5. Top panel: The Fourier transforms of the six lines of the star HR9106. Bottom panel: The vcf-plots of these six lines

with a large rotational velocity of $v_{\rm rot}\sin i$ = 144 km s^{-1}. These lines in this spectrum are highly blended due to rotational broadening; some lines, most noticeably the lines at λ 6265.143 and λ 6270.228, cannot be distinguished anymore. The middle spectrum is of HR 9106 with $v_{\rm rot}\sin i$ = 31.5 km s^{-1}. Here the lines are still clearly distinguishable although some lines are already blending into each other. The bottom spectrum is of HR 7729 with $v_{\rm rot}\sin i$ < 5 km s^{-1}. All lines are separated except the line at λ 6270.228 Å, which shows blending with Fe II λ 6269.982 Å.

3. Determination of projected rotational velocities

The FBT method (Deeming 1975) that we use to determine the rotational velocities has been described in detail in Paper I. With this method one can obtain the projected rotational velocity by means of a successive Fourier-Bessel transformation. The effect of rotation on an intrinsically monochromatic line profile can be calculated (Carrol 1933): for a spherical star without limb darkening, the line profile is half an ellipse. For a star with limb darkening a somewhat more complicated analytical expression can be derived (Carrol 1933). The Fourier transform of this profile is a first-order Bessel function. The rotational velocity information contained in this Bessel function can be extracted by Bessel transforming the Fourier transform: this Fourier-Bessel transform will give a δ-peak when an absorption line is only broadened by rotation. The location of the peak is a direct measure of the rotational velocity. The effect of other broadening mechanisms is to widen the peak in the Fourier- Bessel transform.

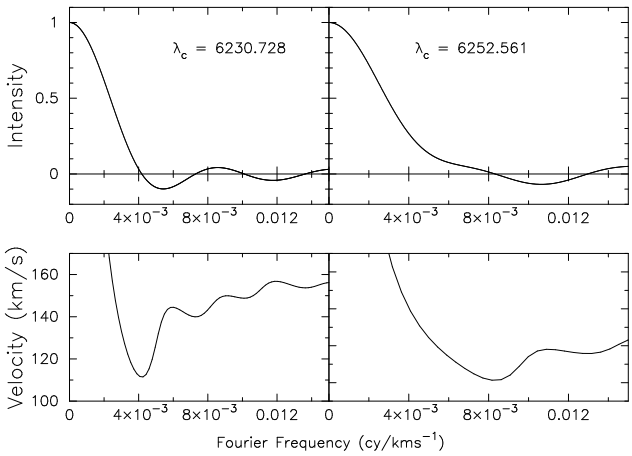

Fig. 6. Top panel: The Fourier transforms of the two lines of the star HR6522. Bottom panel: The vcf-plots of these two lines

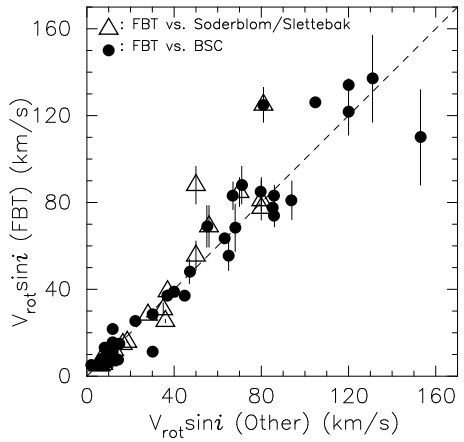

Fig. 7. A comparison of velocities found by the FBT method versus values, found in the literature. For each value also the error bars found with the FBT method are shown. The dashed line is the line of equal rotational velocities

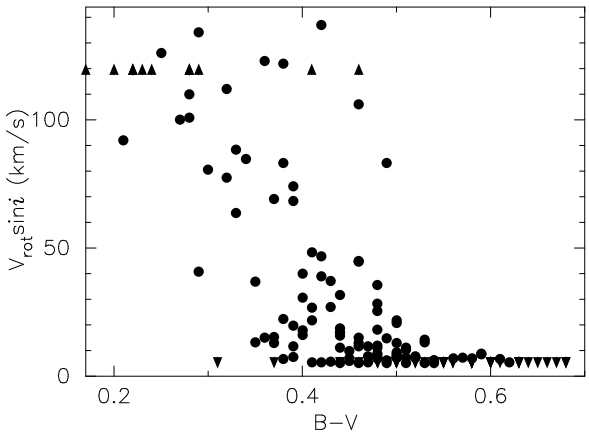

Fig. 9. The rotational velocities versus $B-V$. Triangles indicate upper and lower limits

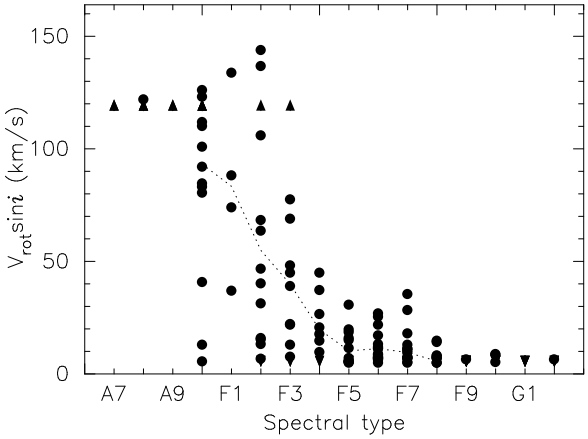

Fig. 8. The rotational velocities per spectral type. The dotted line gives the mean per spectral type. Triangles indicate lower and upper limits

In order to be able to make the Bessel transformation it is necessary, in practice, to choose a frequency up to which the Fourier transform will be used as input of the Bessel transformation. We have found (Paper I) that the value of this cut-off frequency influences the place of the peak in the Bessel transform and therefore the derived rotational velocity. We have solved the problem of where to place the cut-off frequency, by making Bessel transforms with a successively larger part of the Fourier transform as input of the Bessel transform.

When the derived velocity for each Bessel transformation is plotted as a function of its corresponding cut-off frequency, a figure as displayed in the lower panel of Fig. 3 emerges. (This is what we call a 'vcf-plot', 'velocity versus cut-off frequency plot'.) Model calculations as presented in Paper I show that (within 0.4%) the correct rotational velocity is reached at the top of the first local maximum. Therefore, the rotational velocity of a star can be determined from these plots by taking the height of the first local maximum [this occurs at a frequency of $\sim$0.075 cy/(km s^{-1}) in Fig. 3]. As can be seen in Paper I, for this method to give a correct result, the input of the Bessel transformation must extend up to half way between the first and second zero-point in the Fourier transform, which limits the applicability of this method for very low rotational velocities.

The method as we have developed in Paper I starts with an 'ideal picture' of a rotating star. The line shape is only determined by rotation. Initially, no 'disturbing' factors, such as limb darkening, macroturbulence or microturbulence, are taken into account. In Paper I we have investigated the effects of these factors on the derived rotational velocities; we found that the errors introduced by most of these assumptions are generally less than a few percent. The largest systematic error is introduced by the neglect of limb darkening. For an assumed linear limb darkening coefficient, $\beta \sim 0.6$, the neglect of limb darkening results in a systematic underestimation of the rotational velocities by $\sim$5% (see Paper I).

We therefore conclude that this FBT method provides a quick and easy way to determine the rotational velocities of a large sample of stars, with an accuracy of a few percent.

If, apart from rotation, also other parameters of the stellar velocity field are to be determined, the Fourier transformation method, as used extensively and described by Gray (see Gray 1992 for more references), is better suited. One has to keep in mind, however, that Gray's

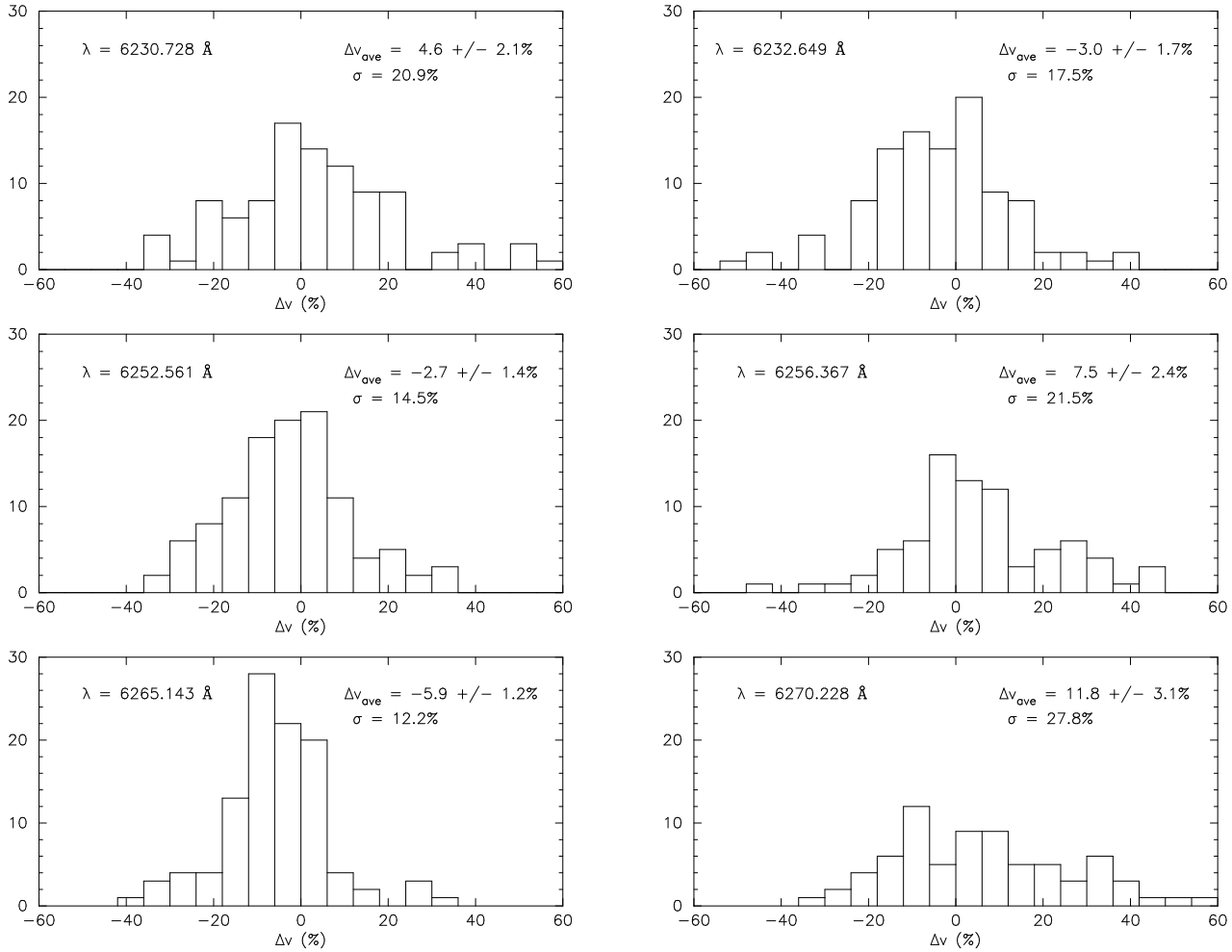

Fig. 10. For each of the six lines used; a histogram of the deviation from the mean for each line in each star

method shares several assumptions with the one we use (e.g sphericity of the star, no effect of rotation on the emitted spectrum) which at some level of accuracy affect the inferred rotational velocities (see, e.g. Collins & Truax 1995).

Limitations to what can be achieved with this method are determined by the spectra used. The lower limit to the accessible velocity range is determined by the spectral resolution. In our case the wavelength bin size is 0.05 Å. From the width of the Th-Ar comparison lines we estimate our resolution to be $\sim$ 2 pixels, i.e. 0.1 Å. Following the results of Paper I the corresponding smallest rotational velocity is 5 km s^{-1}. The upper limit is set by the line density. For the wavelength range we used, severe blending occurred at rotational velocities of more than 90 km s^{-1} (see Fig. 2), resulting in uncertain rotational velocities above this value.

The centers of the lines were chosen at the center of a Gauss fit to the line profile. If a line was blended on one of the two flanks, it was mirrored around its center to get a non-blended, symmetric line. In our analysis, we found that for spectra in which five if the six lines were unblended and the sixth was slightly blended, the rotational velocity derived from this sixth line was always larger when the line was mirrored (up to 30%) compared with the unmirrored value.

This mirroring, however, was kept to a minimum, because due to the uncertainty of the center of the blended line, the mirrored line could, artificially, be made narrower or wider in this way. This is what we found in our analysis. If a star was found in which five of the six lines were unblended and the sixth was slightly blended, the rotational velocity derived from this sixth line always showed a positive deviation when the line was mirrored (up till 30%) compared to the value when it was not mirrored. We conclude that mirroring should be kept to a minimum.

If one of the sides of an absoprtion line is blended with another line, this may affect the derived line center, which is determined by fitting a Gaussian to the line. In general the line center will be replaced towards the blended side. If

subsequently the line is mirrored around the center of the fit, this will result in a line which is too wide and which gives therefore a rotational velocity that is too large. To avoid this problem we have excluded that part of the line which is clearly blended from the Gaussian fit. From inspection by eye, we find that this gives satisfactory results.

From the Gaussian fit to the line one also gets a 1 σ error on the inferred line center. To further investigate the effect of the placement of the line center on the determination of the rotational velocity, we shifted the line center by this 1 σ error towards the blue and the red and calculated the derived rotational velocities with these new line centers. One could take the average of these values as an 'error' on the derived rotational velocity solely due to the placement of the line center. We found that for symmetrical lines this 'center-error' is negligible compared with the spread in rotational velocities one gets from the different lines in one spectrum. In asymmetric or slightly asymmetric lines this 'center-error' becomes larger (which is not surprising since the 1 σ error on the fit to the line center becomes larger), but is in all cases still smaller or comparable to the spread in derived rotational velocities from the different lines.

The highest possible frequency up to which the Fourier transform can be calculated is the Nyquist frequency. However, for fast rotating stars, the relevant information is contained in the low frequencies. If we were to calculate the Fourier transform all the way up to the Nyquist frequency, this relevant information would be contained in only the first few points at low frequencies and would be diluted with noise in the subsequent Bessel transformation. To avoid this, we have made the highest frequency up till which the Fourier transform was calculated, velocity dependent and kept the number of calculated points constant. From the width of the absorption line (indicated by its Full Width at Half Maximum, FWHM), we estimate the frequency at which the first zero-point (u_0) in the Fourier transform would approximately occur (Eq. (1) in Deeming 1975):

$$u_0 = \frac{3.83}{2\,\pi\,\mathrm{FWHM}} \qquad (1)$$

The highest frequency in the Fourier transform was set to six times this frequency u_0. If this highest frequency would be larger than the Nyquist frequency, we have taken the Nyquist frequency as the highest.

In Paper I we have shown that it would be best to determine the rotational velocity in the velocity versus cut-off frequency (vcf) plot at the highest possible a cut-off frequency. However, due to insufficiently high S/N-ratios in most stars, in practice, the rotational velocities have been determined at the first local maximum. This introduces a very small systematic error (0.4%; see Paper I), but in almost all cases, this systematic error is much smaller than the error derived from comparison of different lines in one spectrum.

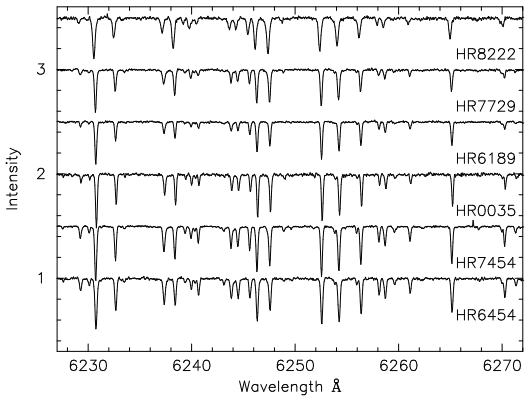

Fig. 11. The reference stars for the convolution method. The spectra have been shifted 0.5 relative to each other

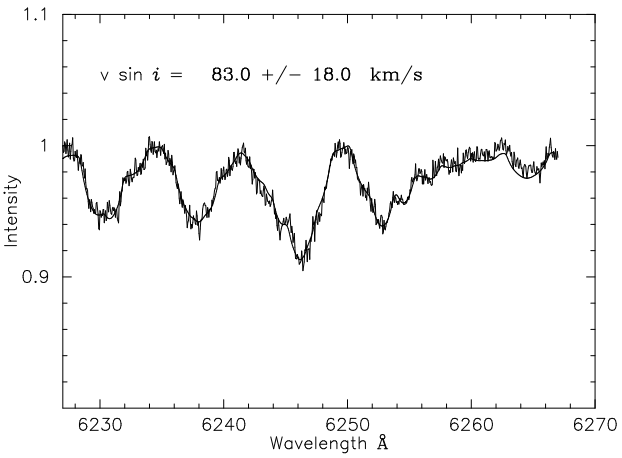

Fig. 12. The target spectrum of HR6093 and its best fit with the convolution method. The errors given are 1 σ errors

To get a feeling of what may be encountered when using the FBT method, we will now show the Fourier transforms and vcf-plots of some representive stars from our sample. These examples demonstrate the way the method works in practice, and also show examples of complicating effects that may occur.

3.1. *Example 1: The majority of cases*

In Fig. 3 the Fourier transforms and vcf-plots for the six lines in the spectrum of HR 7605 are shown. In this plot each column represents the Fourier transform and the vcf-plot of one of the six spectral lines. We find this star to have a rotational velocity of $\sim$ 12 km/s. In all lines the Fourier transform extends to well beyond the first minimum. In the vcf-plots the first local maximum can be well

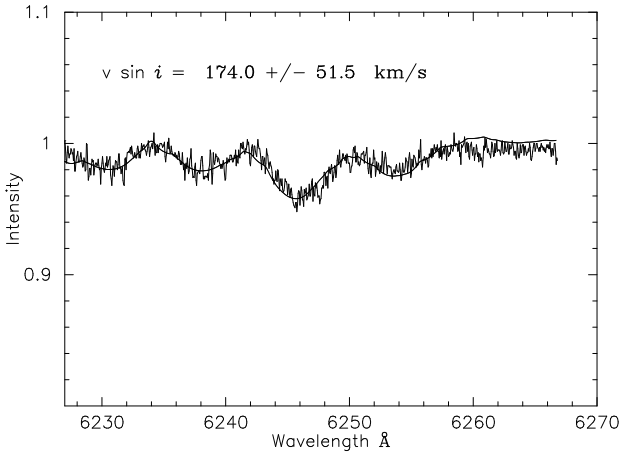

Fig. 13. The target spectrum of HR6507 and its best fit with the convolution method

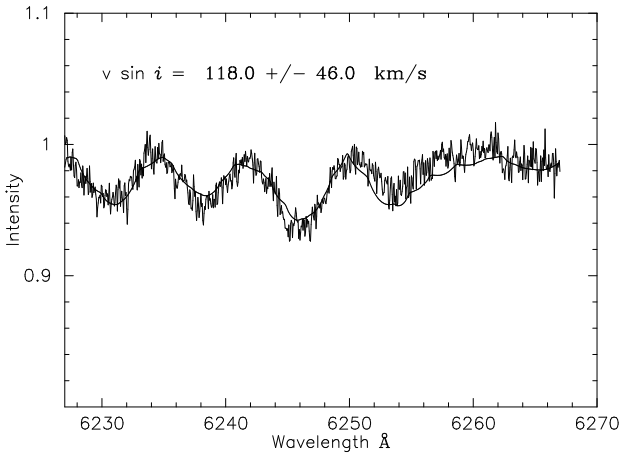

Fig. 14. The spectrum of HR6507 with its best fit. See also Sect. 3.4. The bad fit at wavelengths $> \lambda$ 6250 is caused by an underestimation of the slope of the continuum during the normalization of the spectra

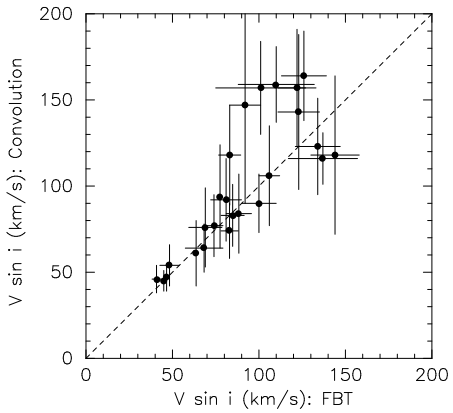

Fig. 15. Comparison between rotational velocities derived by the FBT method and the convolution method. For velocities > 90 km/s the agreement between the two methods is poor, but for velocities < 90 km/s the agreement is good

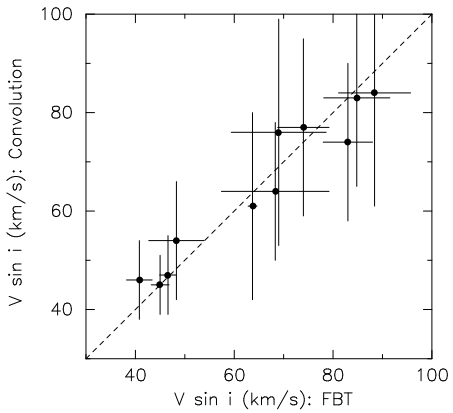

Fig. 16. As Fig. 15, but now only for rotational velocities $<$ 90 km/s

distinguished, but any further maxima are lost in noise. This star is an example of the kind of Fourier transforms and vcf-plots encountered for most stars. From the scatter in the values of $v_{\rm rot}\,\sin i$ for the different lines we find that the rotational velocity can be determined with an average error in the mean of $\sim 5\%$.

3.2. *Example 2: The upper limit*

The star HR 7729 has a rotational velocity below the minimum value that is set by the data spacing. This is clear in the Fourier transforms and vcf plots of Fig. 4. The maximum frequency for which the Fourier transform can be calculated is set by the data spacing. Therefore the Fourier transform cannot be calculated beyond the first zero-point. For some lines, not even this zero-point is reached. The vcf-plots therefore extend only till the first local minimum, but never to the first local maximum. In this case the FBT method is not capable of measuring the rotational velocity. We can only derive an upper limit to $v_{\rm rot}\,\sin i$.

3.3. *Example 3: Low S/N ratios*

In the first three columns of Fig. 5 (HR 9106) we see vcf-plots that somewhat resemble those for stars with limb darkening (see Paper I), i.e. a progressive increase of the height of the local maxima in the vcf-plot. However, this

is not limb darkening, because the ratio of the second to the first maximum ($V_2/V_1 = 1.16$) is much too large. (See Fig. 14 in Paper I.) Because the S/N ratio of the lines is rather low, the vcf-plots are only reliable up to the first local maximum in the vcf plot.

The last column shows the Fourier transform and vcf-plot for the λ 6270.228 line. This line is the weakest of the six and therefore suffers most from a low S/N-ratio. Due to noise, its Fourier transform remains positive at its first local minimum, and only goes through zero at $\sim$0.03 cy/km s^{-1}. This behaviour is reflected in the vcf-plot. The line starts at very high velocities. It then drops down to what should be a local minimum, but instead of recovering and going to the first local maximum, it continues to go down, comes to a second local minimum at $\sim$0.03 cy/km s^{-1} and only then recovers to a local maximum. Clearly this maximum is not a measure of the rotational velocity. From this line therefore no rotational velocity can be determined with the FBT method.

3.4. *Example 4: Line blending*

At high rotational velocities the lines in our spectrum start to blend. HR6522 is an example of such a rapidly rotating star. Figure 6 shows the Fourier transforms and vcf-plots of this star. Only two lines ($\lambda\lambda$ 6230.728 and 6252.561) can be distinguished. The second line can be discarded because in its Fourier transform the same effect is visible as in the λ 6270.228 line of HR 9106 (Fig. 5). However, the vcf-plot of the λ 6230.728 line looks acceptable: even at the highest frequencies, there is no indication of distortion. The rotational velocity derived from this plot would be 144 km/s. However, because of this high rotational velocity, several lines are likely blended. Therefore the values derived from this line should be treated with great caution in spite of the fact that 'it looks nice'. We compare our results for rapidly rotating stars with those obtained using a convolution method in Sect. 5.

4. Results of the FBT method

The results of our analysis are listed in Table 4, which lists the HR number of the stars, $B-V$ colours, spectral type, rotational velocities as determined by us with the FBT method and with the convolution method (see Sect. 5), values that were previously determined by others, and the number of lines used in the determination of the rotational velocity for each star. The errors listed in Table 4 for the FBT method are the rms values of the spread in velocities found for the different lines divided by the square root of the number of lines used in each spectrum. These errors are usually larger than the systematic errors as determined in Paper I. The errors in the values of stars for which more than one line profile could be used, range from $\sim$5% for low velocities up till $\sim$ 10% for high velocities. For some rapidly rotating stars the rotational velocities were determined from one spectral line only. In this case no errors from the spread in velocities in the different lines can be given. The errors for these lines have been set at 10%.

We have looked at the lines seperately, to see if any of the six lines we used gave significantly different rotational velocities. In Fig. 10 we show the distributions of the deviations from the mean rotational velocity, as determined in each star from all the lines, for each of the six lines. The 1 σ error in the distribution is between 12 and 27%. There are no significant systematic effects in the rotational velocities inferred for the individual lines. We see that none of the six lines deviates substantially and systematically from the mean of the lines. The total number of times the line λ 6270.228 was used, is quite a bit less than the others. This is not surprising, since it is the weakest of the six lines and therefore the first to suffer from noise. This an important point to keep in mind, because in the way we have normalized our Fourier transforms (see Paper I), the noise level is not at the same amplitude in the Fourier transforms of the different lines in one star. This can be clearly seen in Fig. 5, where we illustrate the analysis of HR9106. For the lines $\lambda\lambda$ 6256.367 and 6270.228 the noise level is higher than that for the other lines. The noise-dominated Fourier transforms of these two lines are distorted at low frequencies, and therefore no rotational velocities can be derived from them.

Our argument for accepting the mean rotational velocity, based on the remaining four lines, none of the six lines deviate from the average in a systematic way. Of course, when a spectrum is affected by noise, the derived rotational velocities are to be regarded with some caution.

Table 2. Average velocity per spectral type

Spec. type	$< v_{\rm rot} \sin i >$	Spec. type	$< v_{\rm rot} \sin i >$
A7	>100	F5	10 ± 2
A8	>100	F6	10 ± 2
A9	>100	F7	13 ± 4
F0	96 ± 11	F8	< 5
F1	82 ± 10	F9	< 5
F2	57 ± 12	G0	< 5
F3	43 ± 12	G1	< 5
F4	21 ± 5	G2	< 5

In Fig. 7 we compare our results with rotational velocities determined previously. These velocities were taken from the Bright Star Catalogue (Hoffleit & Jaschek 1982) and from Slettebak (1975) and Soderblom (1982). The agreement between our determinations and previous results is generally good, although some stars show large deviations. For rapidly rotating stars ($v \sin i > 90$ km/s) the values derived by us are uncertain.

Table 2 lists the average projected rotational velocity as a function of spectral type. In Figs. 8 and 9 the rotational velocities are plotted versus spectral type and

$B-V$, respectively. The triangles indicate upper and lower limits. The dotted line in Fig. 8 indicates the mean rotational velocity for each spectral type (see Table 2). If we compare these mean values with those found in previous studies, e.g. Huang (1953) or Fukuda (1982), we see that our results are consistent with previous findings for spectral types up to $\sim$ F5. For later spectral types we find values which are, on average, lower by $\sim$50 %. This is mainly due to the fact that many small $v_{\rm rot}\,\sin i$ values in the catalogue of Fukuda are actually upper limits, not measured values.

5. Rotational velocities with a convolution method

Because, due to line blending, for high rotational velocities ($>$ 90 km/s) application of the FBT method becomes difficult, and also in order to have an independent check on the FBT method we have determined the rotational velocities for stars with suspected high rotational velocities in a different way too, using a method described by Danziger & Faber (1972). To measure the rotational velocity of a target star, we consider a star of the same spectral type, for which we know that it has a very low rotational velocity. These slowly rotating stars have been taken from our sample; they are listed in Table 3 and their spectra are shown in Fig. 11. We convolved these reference spectra with the (semi-ellipsoidal) rotational broadening profile (no limb darkening included), for a range of assumed values of $v_{\rm rot}\,\sin i$. This rotational velocity was adjusted to get a best χ^2-fit to the spectrum of the target star. In Figs. 12-14 we show three examples of such fits. The results are also listed in Table 4, Col. 5. The errors given are 1 σ errors, determined from $\Delta\chi^2 = +1$.

Even for very high velocities as in the case of HR 6507, see Fig. 13, this method gives reliable results, although the errors get quite large. All stars with rotational velocities larger than 40 km/s and in whose spectra some evidence of spectral lines were visible have been analysed in this way.

Table 3. Reference stars for convolution method

Spectral type	Reference star
$\leq$ F0	HR8222
F1 + F2	HR7729
F3	HR6189
F4	HR0035
F5	HR7454
F7	HR6454

In Fig. 15, we compare the results obtained with the convolution method with those of the FBT method. For rotational velocities up to $\sim$90 km/s, the agreement between the two methods is very good. We, therefore, conclude that the values, derived by the FBT method from our spectra are not affected by serious systematic effects, except for the neglect of limb darkening.

A comparison with the results of a convolution method shows that for $v_{\rm rot}\,\sin i > 90$ km/s the FBT method gives rotational velocities that are (on average) too small. This is probably an effect of an underestimation of the continuum of the star. In order to make the fits as shown in Figs. 12-14, it was necessary to shift the convolved profile upward to fit to the observed spectrum. This means that in the observed spectrum the continuum was estimated too low, i.e. the tops of the lines were 'chopped' off, resulting in rotational velocities that are too low. Numerical simulations show that un underestimation of the continuum by $\sim$ 25% of the central line depth, which is approximately the value for the spectra with large rotational velocities, will result in an underestimation of the rotational velocity of $\sim$ 10%.

6. Conclusions

We have measured the projected rotational velocities for 178 A, F and G-type stars, with typical uncertainties of $\sim$ 5% for $v_{\rm rot}\,\sin i \leq 40$ km/s to $\sim$ 10% at $v_{\rm rot}\,\sin i$ $\sim$90 km/s, using the method of Fourier-Bessel Transformation, as described in Paper I. Due to line blending we have not been able to determine accurate rotational velocities higher than 90 km/s with the FBT method.

Acknowledgements. We would like to thank the referee for his useful comments. PJG wishes to thank Martin Marinus for his critical reading of the manuscript.

References

Carrol J.A., 1933, MNRAS 93, 478
Carrol J.A, Ingham L.J., 1993, MNRAS 93, 508
Collins G.W. II, Truax R.J., 1995, ApJ 439, 860
Danziger I.J., Faber S.M., 1972, A&A 18, 428
Deeming T.J., 1977, Ap&SS 46, 13
Fukuda I., 1982, PASP 94, 271
Gray D.F., 1981, ApJ 251, 152
Gray D.F., 1982, ApJ 258, 201
Gray D.F., 1989, ApJ 347, 1021
Gray D.F., 1992, The Observation and Analysis of Stellar Photospheres, Cambridge Astrophysics Series, Vol. 20. Cambridge Univ. Press, Cambridge, UK
Herbig G.H., Spelding J.F., 1953, PASP 65, 192
Herbig G.H., Spelding J.F., 1955, ApJ 121, 118
Hoffleit D., Jaschek C., 1982, The Bright Star Catalogue, Yale University Observatory, New Haven, U.S.A.
Huang S., 1953, ApJ 118, 285
Kraft R.P., 1965, ApJ 142, 681
Kurucz R.L., 1979, ApJS 40, 1
Kurucz R.L., 1992, Rev. Mex. Astr. Astroph 23, 45

Kurucz R.L., Peytremann E., 1975, A Table of Semiempirical gf values, SAO special report, No. 362, parts 1-3
Piters A.J.M., Groot P.J., van Paradijs J., 1995, A&A (submitted), (Paper I)
Piters A.J.M, Van Paradijs C.J., Schmitt J.H.M.M., 1995, A&A (in preparation)
Schmitt J.H.M.M., Golub L., Harnden F.R. jr., et al., 1985, ApJ 290, 307
Slettebak A., 1955, ApJ 121, 653
Slettebak A., Collins G.W., Boyce P.B., White N.M., Parkinson T., 1975, ApJS 29, 137
Soderblom D.R., 1982, ApJ 263, 239
Uesugi A., Fukuda I., 1982, Revised Catalogue of Rotational Velocities, Kyoto University, Kyoto, Japan
Walter F.M., 1983, ApJ 274, 794